Published in final edited form as:
Proc SPIE. 2013 March 29; 8672: . doi:10.1117/12.2006492.

Biodistribution Study of Nanoparticle Encapsulated Photodynamic Therapy Drugs Using Multispectral Imaging

Luma V. Halig[1], **Dongsheng Wang**[2], **Andrew Y. Wang**[3], **Zhuo Georgia Chen**[2,*], and **Baowei Fei**[1,4,5,*]

[1]Department of Radiology and Imaging Sciences, Emory University, Atlanta, GA

[2]Department of Hematology and Medical Oncology, Emory University, Atlanta, GA

[3]Ocean NanoTech, LLC, Fayetteville, AK

[4]Department of Biomedical Engineering, Emory University and Georgia Institute of Technology

[5]Department of Mathematics and Computer Science, Emory University

Abstract

Photodynamictherapy (PDT) uses a drug called a photosensitizer that is excited by irradiation with a laser light of a particular wavelength, which generates reactive singlet oxygen that damages the tumor cells. The photosensitizer and light are inert; therefore, systemic toxicities are minimized in PDT. The synthesis of novel PDT drugs and the use of nanosized carriers for photosensitizers may improve the efficiency of the therapy and the delivery of the drug. In this study, we formulated two nanoparticles with and without a targeting ligand to encapsulate phthalocyanines 4 (Pc 4) molecule and compared their biodistributions. Metastatic human head and neck cancer cells (M4e) were transplanted into nude mice. After 2–3 weeks, the mice were injected with Pc 4, Pc 4 encapsulated into surface coated iron oxide (IO-Pc 4), and IO-Pc 4 conjugated with a fibronectin-mimetic peptide (FMP-IO-Pc 4) which binds specifically to integrin β1. The mice were imaged using a multispectral camera. Using multispectral images, a library of spectral signatures was created and the signal per pixel of each tumor was calculated, in a grayscale representation of the unmixed signal of each drug. An enhanced biodistribution of nanoparticle encapsulated PDT drugs compared to non-formulated Pc 4 was observed. Furthermore, specific targeted nanoparticles encapsulated Pc 4 has a quicker delivery time and accumulation in tumor tissue than the non-targeted nanoparticles. The nanoparticle-encapsulated PDT drug can have a variety of potential applications in cancer imaging and treatment.

Keywords

Multispectral imaging; iron oxide; theranostic agent; head and neck cancer; optical imaging; nanoparticles; phthalocyanine 4 (Pc 4); photodynamic therapy; photosensitizers; nanomedicine; pharmaceutical nanocarriers; drug delivery; drug-encapsulation

1. INTRODUCTION

Head and neck cancers account for approximately three percent of all cancers in the United States [1]. Worldly, this type of cancer is accountable for approximately 200,000 deaths yearly [2]. These cancers are nearly twice as common among men as they are among women

*Corresponding authors: gzchen@emory.edu and bfei@emory.edu, Website: www.feilab.org.

[3]. Head and neck cancers are also diagnosed more often among people over age 50 than they are among younger people. More than 52,000 men and women in the United States are expected to be diagnosed with head and neck cancers in 2012 [3]. Regular cancer managements are restricted to chemotherapy, radiation, and surgery. Locoregional recurrence develops in 30% to 40% of patients and distant metastases occur in 20% to 30% of head and neck squamous cell carcinomas (HNSCCs) which is a major factor contributing to poor prognosis and quality of life [4]. Conventional treatments are successful in a narrow subgroup and often leave the patient with disfigurement and permanent undesirable effects on their normal physiologic functions [5]. Surgery and radiation treatment have been exhaustedly used for numerous of these patients and conventional chemotherapy is the only lingering option however, this comes with limited effectiveness and frequent unbearable toxicity. Non-specific distribution of chemotherapy agents cause inadequate drug accumulation in the tumor, off-target attack of normal cells, and unacceptable toxicity, and the limited ability to monitor therapeutic responses, these are the main restriction of the current chemotherapeutic agents [6]. Poor drug delivery to the target site leads to significant complication, such as multidrug resistance [7]. Early detection and superlative treatment are paramount for the improvement of patient survival and care. New therapeutic strategies that show advances in early detection and provide patients with minimum side effect are much in need for head and neck cancer.

Photodynamic therapy (PDT) has emerged as an important therapeutic options in management of cancer [8]. PDT is based on the concept that photosensitizers (PSs) can be preferentially localized in tumor tissue upon systemic administration [9, 10]. When illuminated with an appropriate wavelength of light it then activates the PS resulting in irreversible damage to the tumor cells [10, 11]. In this study, we used PDT for cancer with a second generation PS, the Silicon Phthalocyanine (Pc 4) which is photoactivated at the tissue penetrating wavelength of approximately 672 nm [12]. Pc 4 has a higher molar extinction coefficient which indicates that Pc 4 can efficiently absorb a larger amount of photons at greater tissue depth than the first generation of PSs [12]. Each component is harmless alone; however when combined it can lead to the generation of reactive oxygen species (ROS), oxidative cell damage, and cell death. The administration of such PS usually takes 24 hours or more to accumulate at the tumor site [13]. This creates a risk for toxicity and side effects, for this reason an efficient drug delivery vector is needed. Furthermore, the majority of studies executed on experimental animal species bearing diverse tumor models have shown a high accumulation of PS in the tumor site present a heightened therapeutic potential. The choice of the suitable delivery system for appropriate PS and tumor type is tremendously imperative [10]. PDT has shown to be successful in conjunction with other therapeutic modalities, such as surgery, chemotherapy, and radiotherapy. PDT is a promising alternative for superficial malignant or premalignant lesions of the head and neck [14]. Furthermore, it has shown valuable with recurrent surface disease after surgery or radiotherapy [14].

Nanotechnology has started to transform the scale and methods of drug delivery [15]. Drugs are commonly plagued with tribulations such as poor and inconsistent bioavailability [15]. Innovative advances in nanotechnology have granted researchers with novel tools for cancer imaging and treatment. These advancements have furthermore shown promises of nanoparticles (NPs) for tumor-targeted drug delivery and noninvasive tumor imaging [16, 17]. The development of effective delivery of therapeutic agents may be able to improve patient survival. Iron oxide nanoparticles have a longer blood circulation time than conventional chemotherapeutic drug alone [18]. They are not typically engulfed by the mononuclear phagocytic system (MPS) within the liver or excreted by the kidney, which is a general restriction to the deliverance of small molecular drugs [19]. Numerous varieties of iron oxide (IO) NPs have been used in clinical settings and have proven to be safe for human

use [20]. IO nanoparticles have a long blood-retention time and are generally biodegradable and considered to have low toxicity [21]. A number of studies have shown the uptake of IO NPs by different variety of cell lines, which permits magnetic labeling of the targeted cells [22]. These characteristic of IO NPs provided enormous advantages for in vivo tumor imaging and drug delivery compared with other types of nanoparticles.

Researchers have discussed Integrin β1 expression in head and neck squamous cell carcinoma (HNSCC) [23,33]. Over expression of receptors or antigens in many human cancers can be used to help provide efficient drug uptake using receptor-mediated endocytosis [15]. It has been shown that highly over expression of integrin β1 in metastatic head and neck cancer cell lines [15, 24]. Integrins β1 is crucial for resistance to radiotherapy in head and neck cancer [25]. Fibronectin mimetic peptide (FMP) has been shown to be effectively bound to integrin β1 in vivo and useful as a ligand for targeted therapy.

In this study, we combine PDT drug, IO NPs, and tumor targeting biomarker (FMP-IO-Pc 4) as a novel theranostic agent for cancer imaging and therapy. This will hopefully facilitate reduction of unwanted toxicity and to further aid in the management of localized tumors, such as residual or recurrent, squamous cell carcinomas (SCC) of the oral cavity, pharynx, larynx, and derma.

2. METHODS AND EXPERIMENTAL DESIGN

2.1 Pc 4 formulation

Pc 4 preparation was previously reported by us [11, 26–29]. Briefly, a stock solution (1 mg/mL) was made by dissolving Pc 4 in 50% Cremophor EL (Sigma-Aldrich) and 50% absolute ethanol and then adding 9 volumes of normal saline with mixing. For injection, the Pc 4 stock solution was mixed with an equal volume of 5% Cremophor EL, 5% ethanol, and 90% saline. Each animal was weighed at the time of injection, and the volume of injected solution was adjusted to provide 0.4 mg/kg for each mouse. The IO NPs were synthesized by Ocean NanoTech, LLC (Fayetteville, AK). The same Pc 4 dose was used for each animal.

2.2 Animal xenograft Model

The HNSCC cells (M4E) were maintained as a monolayer culture in Dulbecco's modified Eagle's medium (DMEM)/F12 medium (1:1) supplemented with 10% fetal bovine serum (FBS) [15,30]. Animal experiments were approved by the Animal Care and Use Committee of Emory University. Twenty four Female Foxn1nu mice (athymic nu/nu, from Harlan Laboratories) aged 4–6 weeks were injected with 2×10^6 M4E cells 2–3 weeks prior to drug injections. Mice were randomized into four groups with equal average tumor size. PBS, Pc 4, IO-Pc4 and FMP-IO-Pc4 at the dose of 0.4 mg/kg body weight were systemically given, respectively when tumor volume reached 100 mm^3. Major organs including lung, liver, heart, spleen, and kidney were collected for hematoxylin–eosin staining and imaging.

2.2 In Vivo Multispectral Imaging

Mice were imaged using CRi Maestro imaging system (Caliper, Hopkinton, MA). During imaging acquisitions, the animals were anesthetized with a continuous supply of 2% isoflurane in oxygen. After the full body scan, mice were euthanized and organs including lung, heart, brain, liver, spleen, kidney, muscle, and skin were gathered; and images were captured. CRi Maestro systems can acquire full multispectral data with down to 25 micron/pixel resolution in only a few seconds. The CRi's spectral imaging system manufactures x-amount of images, where x is user-defined. Each image set contains the measurement of the spectrum of the complete points which comprise it. An orange excitation filter (586 nm – 601 nm) and a 680-nm long-pass emission filter (640 nm – 820 nm) were used to obtain

images from 640 nm to 900 nm in 10-nm wavelength increments. Images were captured at constant increments for four different studies. Using the in-vivo spectral library for Pc 4, IO-Pc 4, or FMP-IO-Pc 4 and the background autofluorescence, a spectral unmixing algorithm was applied to composite images to determine the intensity and location of the drugs. The signal at each pixel of a region of interest (ROI) was obtained in a grayscale representation of unmixed images. The mean signals of the ROIs were calculated and analyzed. To determine whether the difference between these means were statistically significant, an unpaired student's t-test was performed.

3. RESULTS

3.1 Biodistribution comparison between Pc 4 and IO-Pc 4

Images were acquired at pre-injection and 1, 30, and 150 minutes post injection. All images were analyzed and the results are shown in Figure 1. The graph indicates a high average accumulation of the Pc 4 encapsulated NPs as compared to the non-conjugated Pc 4 at the tumor tissues. This data demonstrates that the delivery of Pc 4 in vivo is enhanced when delivered by IO NPs.

3.2 Biodistribution comparison of Pc 4, IO-Pc 4, FMP-IO-Pc 4

In another experiment, images were acquired at pre-injection and 1, 4, 24, and 48 hours post injection. In addition, mice were sacrificed, dissected, and the organs were removed for scanning. Mouse organ scans were captured using the same in vivo imaging parameters. Multispectral un-mixing shows an increased accumulation of FMP-IO-Pc 4 than both free Pc 4 and the non-targeted nanoparticle IO-Pc 4. The result data show that the highest intensity was seen in the liver, kidney, and lungs and the lowest in the heart, spleen, and brain. Accumulate in the lungs has been seen after injection of large amounts of Pc 4. This has been described in [31] as the mode of dark dose-limiting toxicity.

Ex-vivo quantitative results between Pc 4, IO-Pc 4, and FMP-IO-Pc 4 at the tumor site at 4, 24, and 48 hours showed that at 4 hours and 24 hours the signal for FMP-IO-Pc 4 illustrates a significant increase in the average signal count compared to both Pc 4 and IO-Pc 4. Furthermore, FMP-IO-Pc 4 demonstrated an increase at 48 hours however, not to the extent as the previous time points. It has been previously reported that nanoparticle compounds can be removed from the circulation after administration by macrophage of the reticuloendothelial system [32]. Our data showed that FMP-IO-Pc 4 had a higher accumulation compared to the other drugs at 24 hours.

The organ biodistribution analyses show more enhanced signals in the tumor, heart, lung, spleen, liver, kidney, muscle, skin, and brain of the mice that were injected with FMP-IO-Pc 4 compared to those mice that were injected with either Pc 4 or IO-Pc 4. All three drugs demonstrated higher signals in the kidney and liver compared to the tumor, heart, spleen, muscle, skin, and brain. It also showed a higher lung accumulation in all mice with all the three drugs.

4. DISCUSSION AND CONCLUSION

This study demonstrates that nanoparticle encapsulated photodynamic therapy drugs, i.e. IO-Pc 4 and FMP-IO-Pc 4 had an advanced accumulation in the xenografted mouse tumors than the free drug i.e. Pc 4. This study indicates that nanoparticle-based PDT drugs may be able to increase therapeutic efficacy with a low drug dose for the treatment of tumors and that a targeted nanoparticle might show an attractive strategy for enhancement of delivery of the drug to cancer cells, thereby, keeping them away from healthy tissue and thus reducing toxic effects. Our multispectral imaging and analysis methods can be used not only for cancer

detection [34–35] but also for in vivo biodistribution studies. Our previous research on this PDT drug Pc 4 has demonstrated the feasibility of Pc 4-based PDT for prostate cancer [36–40]. This therapy may also be able to treat head and neck cancer.

Acknowledgments

This research is supported in part by NIH grant R01CA156775 (PI: Fei), Georgia Cancer Coalition Distinguished Clinicians and Scientists Award (PI: Fei), and the Emory Molecular and Translational Imaging Center (NIH P50CA128301).

References

1. Jemal A, Siegel R, Xu J, et al. Cancer statistics, 2010. CA Cancer J Clin. 2010; 60(5):277–300. [PubMed: 20610543]
2. Jemal A, Bray F, Center MM, et al. Global cancer statistics. CA: A Cancer Journal for Clinicians. 2011; 61(2):69–90. [PubMed: 21296855]
3. American Cancer Society. Cancer Facts and Figures 2012. Atlanta: American Cancer Society; 2012.
4. Forastiere AA, Goepfert H, Maor M, et al. Concurrent chemotherapy and radiotherapy for organ preservation in advanced laryngeal cancer. N Engl J Med. 2003; 349(22):2091–8. [PubMed: 14645636]
5. Wise-Draper TM, Draper DJ, Gutkind JS, et al. Future directions and treatment strategies for head and neck squamous cell carcinomas. Translational Research. 2012; 160(3):167–177. [PubMed: 22683420]
6. Weeks JC, Catalano PJ, Cronin A, et al. Patients' expectations about effects of chemotherapy for advanced cancer. N Engl J Med. 2012; 367(17):1616–25. [PubMed: 23094723]
7. Gottesman MM, Fojo T, Bates SE. Multidrug resistance in cancer: role of atp-dependent transporters. Nature Reviews Cancer. 2002; 2(1):48.
8. Triesscheijn M, Baas P, Schellens JH, et al. Photodynamic therapy in oncology. Oncologist. 2006; 11(9):1034–44. [PubMed: 17030646]
9. Fei BW, Chen X, Meyers JD, et al. In Vivo Small Animal Imaging for Early Assessment of Therapeutic Efficacy of Photodynamic Therapy for Prostate Cancer. Proceedings of SPIE. 2007; 6511:651102-1–8.
10. Konan YN, Gurny R, Allemann E. State of the art in the delivery of photosensitizers for photodynamic therapy. Journal of Photochemistry and Photobiology B-Biology. 2002; 66(2):89–106.
11. Cheng Y, Samia AC, Meyers JD, Panagopoulos I, Fei BW, Burda C. Highly efficient drug delivery with gold nanoparticle vectors for in vivo photodynamic therapy of cancer. Journal of the American Chemical Society. 2008; 130(32):10643–10647. [PubMed: 18642918]
12. Baron ED, Malbasa CL, Santo-Domingo D, et al. Silicon Phthalocyanine (Pc 4) Photodynamic Therapy Is a Safe Modality for Cutaneous Neoplasms: Results of a Phase 1 Clinical Trial. Lasers in Surgery and Medicine. 2010; 42(10):728–735. [PubMed: 21246576]
13. Dolmans DE, Fukumura D, Jain RK. Photodynamic therapy for cancer. Nat Rev Cancer. 2003; 3(5):380–7. [PubMed: 12724736]
14. Nyst HJ, Tan IB, Stewart FA, et al. Is photodynamic therapy a good alternative to surgery and radiotherapy in the treatment of head and neck cancer? Photodiagnosis and Photodynamic Therapy. 2009; 6(1):3–11. [PubMed: 19447366]
15. Zhang X, Su L, Pirani A, et al. Understanding metastatic SCCHN cells from unique genotypes to phenotypes with the aid of an animal model and DNA microarray analysis. Clinical and Experimental Metastasis. 2006; 23(3):209–222. [PubMed: 17028921]
16. Lee JH, Huh YM, Jun YW, et al. Artificially engineered magnetic nanoparticles for ultra-sensitive molecular imaging. Nat Med. 2007; 13(1):95–9. [PubMed: 17187073]
17. Farokhzad OC, Karp JM, Langer R. Nanoparticle-aptamer bioconjugates for cancer targeting. Expert Opin Drug Deliv. 2006; 3(3):311–24. [PubMed: 16640493]

18. Wahajuddin, Arora S. Superparamagnetic iron oxide nanoparticles: magnetic nanoplatforms as drug carriers. International Journal of Nanomedicine. 2012; 7:3445–3471. [PubMed: 22848170]
19. Gaucher G, Dufresne MH, Sant VP, et al. Block copolymer micelles: preparation, characterization and application in drug delivery. J Control Release. 2005; 109(1–3):169–88. [PubMed: 16289422]
20. Hamm B, Staks T, Taupitz M, et al. Contrast-enhanced MR imaging of liver and spleen: first experience in humans with a new superparamagnetic iron oxide. Journal of Magnetic Resonance Imaging. 1994; 4(5):659–68. [PubMed: 7981510]
21. Moore A, Weissleder R, Bogdanov A Jr. Uptake of dextran-coated monocrystalline iron oxides in tumor cells and macrophages. Journal of Magnetic Resonance Imaging. 1997; 7(6):1140–5. [PubMed: 9400860]
22. Lewin M, Carlesso N, Tung CH, et al. Tat peptide-derivatized magnetic nanoparticles allow in vivo tracking and recovery of progenitor cells. Nat Biotechnol. 2000; 18(4):410–4. [PubMed: 10748521]
23. Choi P, Chen C. Genetic expression profiles and biologic pathway alterations in head and neck squamous cell carcinoma. Cancer. 2005; 104(6):1113–1128. [PubMed: 16092115]
24. Zhang X, Liu YN, Gilcrease MZ, et al. A lymph node metastatic mouse model reveals alterations of metastasis-related gene expression in metastatic human oral carcinoma sublines selected from a poorly metastatic parental cell line. Cancer. 2002; 95(8):1663–1672. [PubMed: 12365014]
25. Eke I, Deuse Y, Hehlgans S, et al. beta(1) Integrin/FAK/cortactin signaling is essential for human head and neck cancer resistance to radiotherapy. Journal of Clinical Investigation. 2012; 122(4): 1529–1540. [PubMed: 22378044]
26. Fei BW, Wang HS, Wu CY, et al. Choline PET for Monitoring Early Tumor Response to Photodynamic Therapy. Journal of Nuclear Medicine. 2010; 51(1):130–138. [PubMed: 20008981]
27. Fei BW, Wang H, Meyers JD, et al. High-field magnetic resonance imaging of the response of human prostate cancer to Pc 4-based photodynamic therapy in an animal model. Lasers in Surgery and Medicine. 2007; 39(9):723–730. [PubMed: 17960753]
28. Wang H, Fei BW. Diffusion-weighted MRI for monitoring tumor response to photodynamic therapy. J Magn Reson Imaging. 2010; 32(2):409–17. [PubMed: 20677270]
29. Fei BW, Muzic RF, Flask C, Wilson DL, Duerk JL, Feyes DK, Oleinick NL. Deformable and rigid registration of MRI and microPET images for photodynamic therapy of cancer in mice. Medical Physics. 2006; 33(3):753–760. [PubMed: 16878577]
30. Rahman MA, Amin ARMR, Wang X, et al. Systemic delivery of siRNA nanoparticles targeting RRM2 suppresses head and neck tumor growth. Journal of Controlled Release. 2012; 159(3):384–392. [PubMed: 22342644]
31. Egorin MJ, Zuhowski EG, Sentz DL, et al. Plasma pharmacokinetics and tissue distribution in CD2F1 mice of Pc4 (NSC 676418), a silicone phthalocyanine photodynamic sensitizing agent. Cancer Chemotherapy and Pharmacology. 1999; 44(4):283–294. [PubMed: 10447575]
32. Chatterjee DK, Fong LS, Zhang Y. Nanoparticles in photodynamic therapy: An emerging paradigm. Advanced Drug Delivery Reviews. 2008; 60(15):1627–1637. [PubMed: 18930086]
33. Wang D, Müller S, Amin AR, et al. The Pivotal Role of Integrin β1 in Metastasis of Head and Neck Squamous Cell Carcinoma. Clinical Cancer Res. 2012; 18(17):4589–4599. [PubMed: 22829201]
34. Akbari H, Halig LV, Zhang HZ, Wang DS, Chen ZG, Fei BW. Detection of cancer metastasis using a novel macroscopic hyperspectral method. Proc SPIE. 2012; 8317:831711–1. [PubMed: 23336061]
35. Akbari H, Halig LV, Schuster DM, Osunkoya A, Master VA, Nieh PT, Chen GZ, Fei BW. Hyperspectral imaging and quantitative analysis for prostate cancer detection. Journal of Biomedical Optics. 2012; 17:076005. [PubMed: 22894488]
36. Cheng Y, Samia AC, Meyers JD, Panagopoulos I, Fei BW, Burda C. Highly efficient drug delivery with gold nanoparticle vectors for in vivo photodynamic therapy of cancer. Journal of the American Chemical Society. 2008; 130:10643–10647. [PubMed: 18642918]
37. Fei BW, Muzic RF, Lee Z, et al. Registration of micro-PET and high-resolution MR images of mice for monitoring photodynamic therapy. Proceedings of SPIE. 2004; 5369:371–379.

38. Fei BW, Wang H, Muzic RF, et al. Finite element model-based tumor registration of microPETand high-resolution MR images for photodynamic therapy in mice. Proceeding of SPIE. 2006; 6143:61433I-1–10.

39. Wang H, Feyes DK, Mulvihill JW, Oleinick NL, MacLennan G, Fei BW. Multiscale fuzzy C-means image classification for multiple weighted MR images for the assessment of photodynamic therapy in mice. Proceedings of SPIE. 2007; 6512:65122W-1–9.

40. Fei BW, Wang H, Chen X, Meyers J, Mulvilhill JW, Feyes DK, Edgehouse N, Duerk JL, Pretlow TG, Oleinick NL. In vivo small animal imaging for early assessment of therapeutic efficacy of photodynamic therapy for prostate cancer. Proceedings of SPIE. 2007; 6511:651102-1–8.

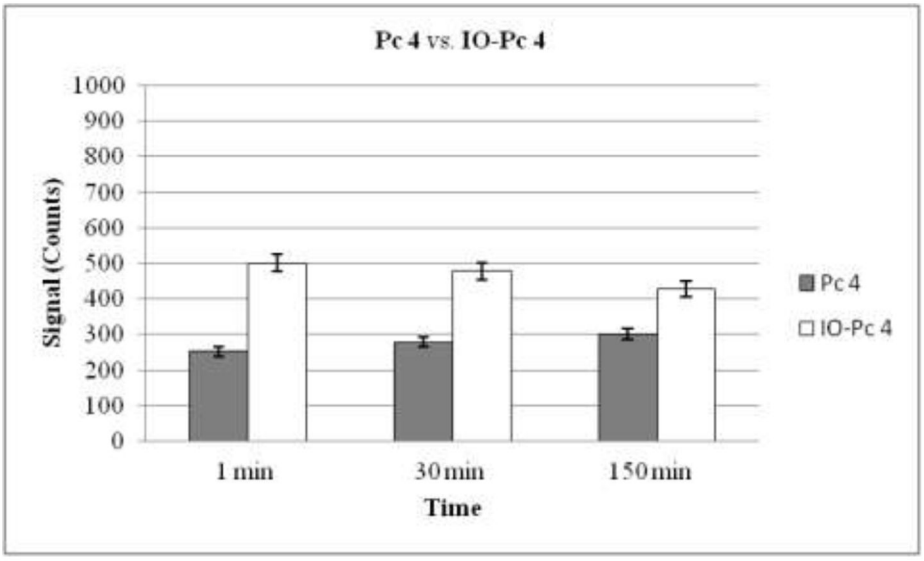

Figure 1.
Biodistribution of Pc 4 versus IO-Pc 4 at 1, 30, and 150 minutes. Each bar represents 6 mice and the error bar is the standard deviation.

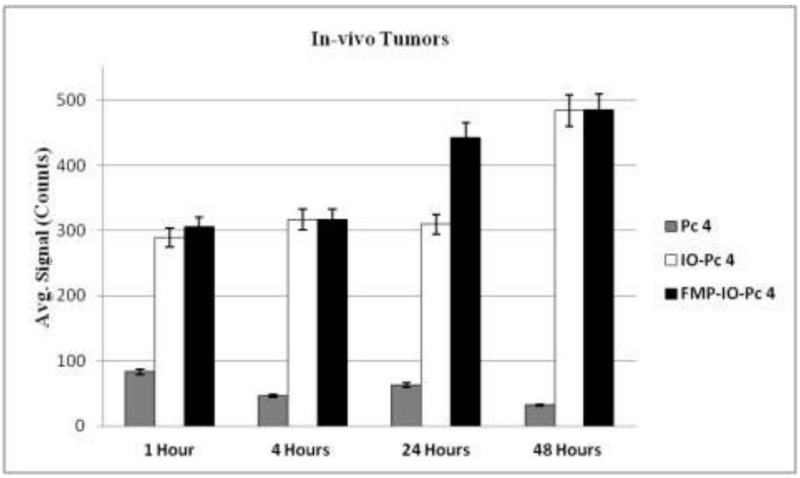

Figure 2.
Biodistribution of Pc 4 versus IO-Pc 4, and FMP-IO-Pc 4 at 1, 4, 24 and 48 hours. Each bar represents 6 mice and the error bar is the standard deviation.

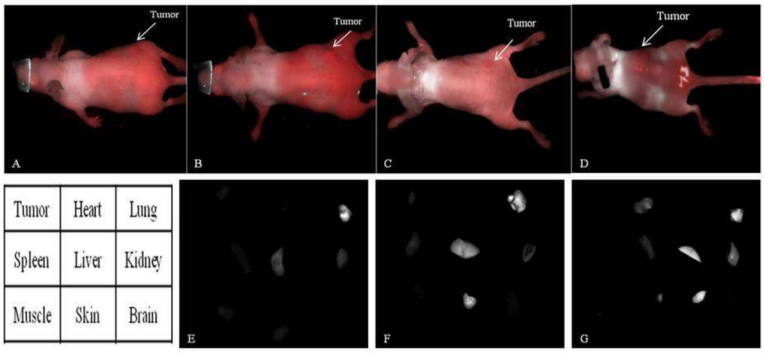

Figure 3.

In vivo images of the mice after Pc 4 injection (top) and the ex-vivo images of the organs after dissection. A. 1 hour (Mouse 108), B. 4 hours (Mouse 108), C. 24 hours (Mouse 117), D. 48 hours (Mouse 116). Each mouse was sacrificed and the organs were dissected for imaging. E. 4 hours (Organs of Mouse 108), F. 24 hours (Organs of Mouse 117), G. 48 hours (Organs of Mouse 116).

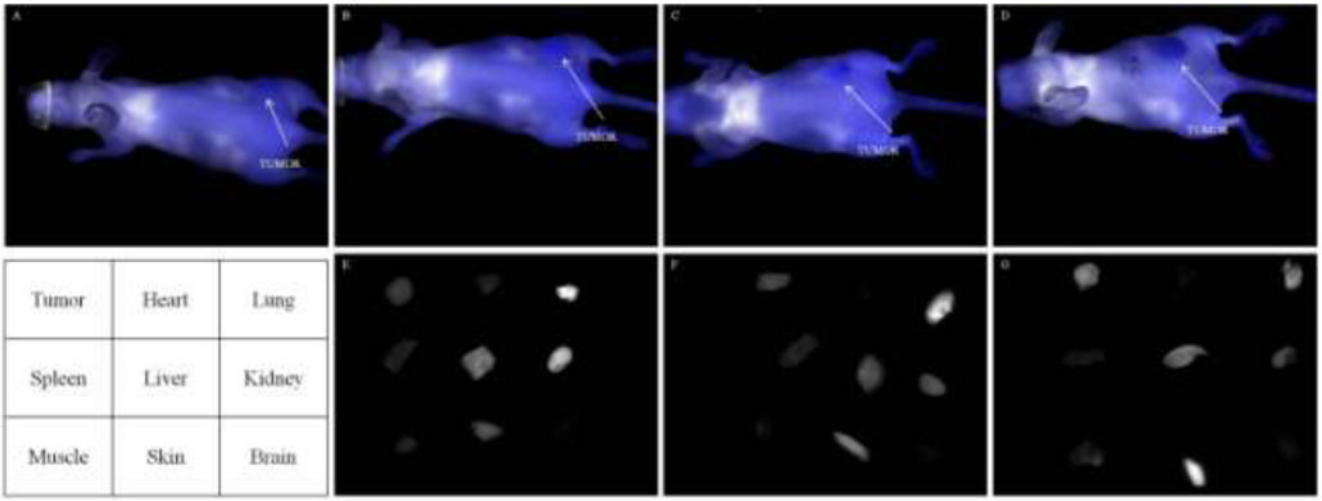

Figure 4.
In vivo images of the mice after IO-Pc 4 injection (top) and the ex-vivo images of the organs after dissection. A. 1 hour (Mouse 103), B. 4 hours (Mouse 03), C. 24 hours (Mouse 146), D. 48 hours (Mouse 150). Each mouse was sacrificed and the organs were dissected for imaging. E. 4 hours (Organs of Mouse 103), F. 24 hours (Organs of Mouse 146), G. 48 hours (Organs of Mouse 149).

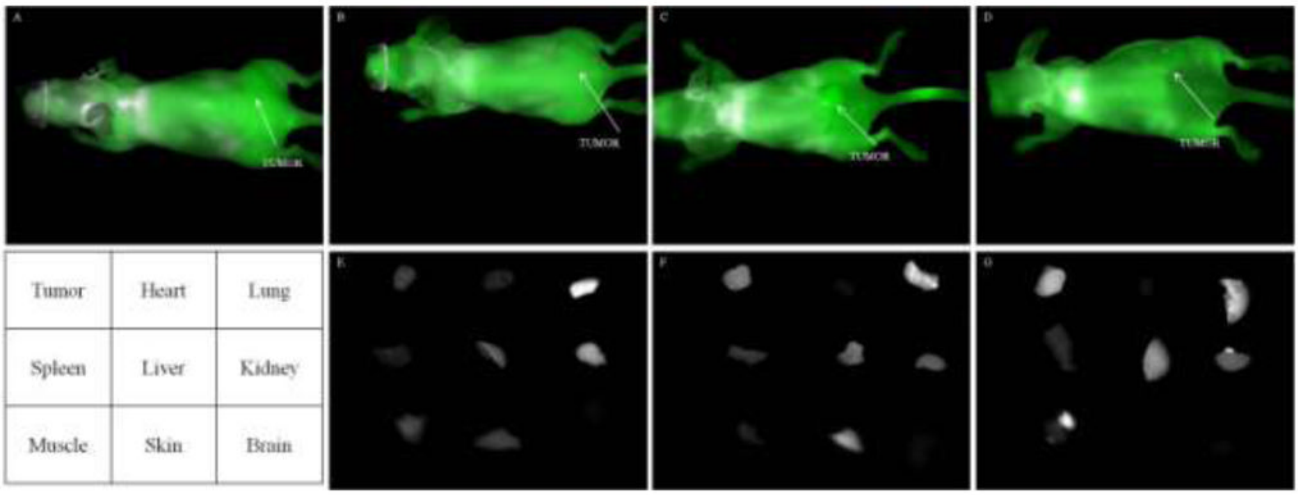

Figure 5.

In vivo images of the mice after FMP-IO-Pc 4 injection (top) and the ex-vivo images of the organs after dissection.. A. 1 hour (Mouse 199), B. 4 hours (Mouse 105), C. 24 hours (Mouse 113), D. 48 hours (Mouse 123). Each mouse was sacrificed and the organs were dissected for imaging. E. 4 hours (Organs of Mouse 199), F. 24 hours (Organs of Mouse 144), G. 48 hours (Organs of Mouse 110).